tilled (HT) and the forest systems were each replicated as three separate sites within 2 km of the other systems on the same or similar soil series. See note 2 in supplemental materials (*28*) for additional site histories.
11. A. J. Franzluebbers and J. L. Steiner, *Adv. Soil Sci.*, in press.
12. E. A. Paul, K. A. Paustian, E. T. Elliott, C. V. Cole, Eds., *Soil Organic Matter in Temperate Ecosystems: Long-Term Experiments in North America* (Lewis CRC, Boca Raton, FL, 1997).
13. G. P. Livingston and G. L. Hutchinson, in *Biogenic Trace Gases: Measuring Emissions from Soil and Water*, P. A. Matson and R. C. Harriss, Eds. (Blackwell, Oxford, 1995), pp. 14–51.
14. Gas sampling protocols appear in note 6 in supplemental materials (*28*).
15. For mean values and statistical details, see Web tables (*28*).
16. Biweekly inorganic N analyses show high levels of N in all cropping systems in late spring. More inorganic N occurs in the conventional systems than in the organic-based systems, but the increase persists several weeks longer in the organic-based systems.
17. IPCC, OECD, IEA, *Revised 1996 IPCC Guidelines for National Greenhouse Gas Inventories* (Organization for Economic Cooperative Development, Paris, 1997).
18. A. R. Mosier *et al.*, *Nutr. Cycl. Agroecosyst.* **52**, 225 (1998).
19. The average daily N_2O flux in our conventional cropping system (3.22 g N_2O-N ha^{-1} day^{-1}) extrapolates to 1.17 kg N_2O-N ha^{-1} $year^{-1}$. Of this, 0.37 to 0.53 kg N_2O-N is apparent background flux (based on fluxes in our successional systems), or 31 to 45% of the 1.17 kg N total. Over a 3-year corn-soybean-wheat rotation in this system, IPCC methodology (*17*, *18*) calculates our N inputs to average 139 kg ha^{-1} $year^{-1}$, for a calculated emission factor of 0.0055 to 0.0067 kg N_2O-N per kg N input, within the lower portion of the IPCC range of 0.0025 to 0.0225.
20. J. T. Houghton *et al.*, *Climate Change 1995* (Cambridge Univ. Press, New York, 1996).
21. We calculated GWP using IPCC factors of 1 for CO_2, 280 for N_2O, and 56 for CH_4 (*20*). Calculation details for all GWP sources appear in Web tables (*28*).
22. Soil carbon storage in surface horizons provides a conservative estimate of in situ CO_2 sequestration for cropped systems. Ignored are potential changes in dissolved C leached to groundwater, changes in soil C deeper in the profile due to root decomposition, and erosion transfers to reservoir sediments. Also uncounted is C captured by woody biomass in our poplar and successional systems because we expect that this C will be oxidized when the wood is eventually harvested.
23. U.S. Department of Agriculture (USDA), *Agricultural Resources and Environmental Indicators, 1996-97* (USDA, Economic Research Service, Washington, DC, 1997).
24. G. Marland, T. A. Boden, R. J. Andres, A. L. Brenkert, C. Johnston, "Global, regional, and national CO_2 emissions," in *Trends: A Compendium of Data on Global Change* (Carbon Dioxide Information Analysis Center, Oak Ridge National Laboratory, U.S. Department of Energy, Oak Ridge, TN, 1999), available at http://cdiac.esd.ornl.gov/trends/emis/tre_usa.htm.
25. P. A. Matson, R. Naylor, I. Ortiz-Monasterio, *Science* **280**, 112 (1998).
26. G. P. Robertson, in *Ecology in Agriculture*, L. Jackson, Ed. (Academic Press, New York, 1997), pp. 347–365.
27. R. A. Houghton, J. L. Hackler, K. T. Lawrence, *Science* **285**, 574 (1999).
28. Supplemental material is available at www.sciencemag.org/feature/data/1051816.shl.
29. G. P. Robertson, C. S. Bledsoe, D. C. Coleman, P. Sollins, Eds., *Standard Soil Methods for Long-Term Ecological Research* (Oxford Univ. Press, New York, 1999).
30. Protocols for NPP and soil N and C follow (*29*); for details, see note 3 in supplemental materials (*28*).
31. This work was supported by the USDA National Research Initiative Program, the Department of Energy National Institute for Global Environmental Change Program, the NSF LTER Program, and the Michigan Agricultural Experiment Station. We thank S. J. Halstead, K. D. Baergen, A. T. Corbin, C. M. Easley, and G. R. Ponciroli for technical assistance in the field and laboratory, M. A. Halvorson for agronomic management, and C. P. McSwiney for fuel use calculations. We also thank A. R. Mosier, K. A. Smith, and P. M. Vitousek for many insightful comments on an earlier draft.

2 May 2000; accepted 28 July 2000

Signal Transduction Through Prion Protein

S. Mouillet-Richard,[1]* M. Ermonval,[1] C. Chebassier,[1,2] J. L. Laplanche,[2] S. Lehmann,[3] J. M. Launay,[2] O. Kellermann[1]

The cellular prion protein PrP^c is a glycosylphosphatidylinositol-anchored cell-surface protein whose biological function is unclear. We used the murine 1C11 neuronal differentiation model to search for PrP^c-dependent signal transduction through antibody-mediated cross-linking. A caveolin-1–dependent coupling of PrP^c to the tyrosine kinase Fyn was observed. Clathrin might also contribute to this coupling. The ability of the 1C11 cell line to trigger PrP^c-dependent Fyn activation was restricted to its fully differentiated serotonergic or noradrenergic progenies. Moreover, the signaling activity of PrP^c occurred mainly at neurites. Thus, PrP^c may be a signal transduction protein.

Although much progress has been made over the past few years regarding the involvement of the scrapie prion protein (PrP^{Sc}) in transmissible spongiform encephalopathies (TSEs) (*1*), the biological function of the cellular, nonpathogenic isoform of PrP, PrP^c, still remains enigmatic. PrP^c is an ubiquitous glycoprotein expressed strongly in neurons (*2*). PrP-deficient mice are viable and develop normally, but they display minor defects that differ according to the null strain (*3*). In contrast, mice expressing an NH_2-terminally truncated version of PrP^c in a null background show neuronal degeneration soon after birth, suggesting that PrP^c may play an important role in the maintenance and/or regulation of neuronal functions (*4*). Recent data have focused on the copper-binding ability of PrP^c (*5*), and an involvement of PrP^c in the regulation of the presynaptic copper concentration and of synaptic transmission has been proposed (*6*). The attachment of PrP^c to the plasma membrane through a glycosylphosphatidylinositol (GPI) anchor may also be consistent with a role in cell-surface signaling or cell adhesion. Indeed, the 37-kD laminin receptor binds PrP^c (*7*).

Because PrP^c may act as a cell-surface receptor, we investigated whether signal transduction pathways coupled to PrP^c after antibody-mediated cross-linking (*8*). Our experimental strategy relies on the neuronal differentiation model 1C11 (*9*). The 1C11 clone is a committed neuroectodermal progenitor with an epithelial morphology that lacks neuron-associated functions (*9*). Upon induction, 1C11 cells develop a neural-like morphology, acquire neuronal markers, and convert into either $1C11^{*/5\text{-HT}}$ (serotonergic) cells or $1C11^{**/NE}$ (noradrenergic) cells. The choice between the two differentiation pathways depends on the set of inducers used (*9*). Within 4 days, $1C11^{*/5\text{-HT}}$ cells implement a complete serotonergic phenotype, including 5-HT synthesis, storage, transport, catabolism, as well as three functional serotonergic receptors of the $5\text{-HT}_{1B/D}$, 5-HT_{2B}, and 5-HT_{2A} subtypes (*9*). The noradrenergic phenotype of $1C11^{**/NE}$ cells is complete within 12 days, with a progressive onset of catecholamine synthesis, storage, transport, catabolism, and an α_{1D}-adrenoceptor (*9*). The differentiation events involve almost 100% of the cells and follow a well-characterized time course.

PrP^c is constitutively expressed in the 1C11 progenitor and throughout differentiation (*10*). Thus, the 1C11 cell line offers the opportunity to study PrP^c in relation to the onset of neuronal functions and within an integrated neuronal context. The effects of antibody-mediated ligation of PrP^c at the cell surface of the 1C11 progenitor or its fully differentiated $1C11^{*/5\text{-HT}}$ and $1C11^{**/NE}$ progenies were followed. PrP^c cross-linking did not induce any specific phosphoinositide (PI) hydrolysis or nitric oxide production, nor did it promote the activation of p21ras or phospholipase A2 in the 1C11 cell line within 30 min of cross-linking (*11*). In contrast, ligation of PrP^c with specific antibodies induced a marked decrease in the phosphorylation level of the tyrosine kinase Fyn in

[1]Différenciation Cellulaire, CNRS–Institut Pasteur, 75724 Paris Cedex 15, France. [2]CR Claude Bernard, Service de Biochimie, Hôpital Lariboisière, 75009 Paris, and Faculté de Pharmacie, 75005 Paris, France. [3]IGH du CNRS, UPR 1142, 34396 Montpellier Cedex 5, France.

*To whom correspondence should be addressed. E-mail: srichard@pasteur.fr

both 1C11*/5-HT and 1C11**/NE cells (Fig. 1A). The effect became measurable 10 min after antibody-mediated ligation. Similar decreases were obtained with two distinct antibodies to PrP (1A8 and SAF 61), but not with irrelevant antibodies directed against the membranous serotonin transporter. Fyn immunoprecipitates were subjected to immune complex kinase assay. As expected (*12*), the dephosphorylation of Fyn monitored in 1C11*/5-HT and 1C11**/NE cells after PrP^c cross-linking increased kinase activity (Fig. 1B). The activation of the Fyn kinase was abolished in the presence of competing Fab fragments of SAF61 antibodies (Fig. 1B).

In 1C11 precursor cells, the phosphorylation level of the tyrosine kinase Fyn was not sensitive to PrP^c cross-linking (Fig. 1A). However, 1C11 cells contain similar amounts of PrP^c as found in 1C11**/NE cells (*10*). Also, PrP^c is equally well released by PI-specific phospholipase C (PI-PLC) from undifferentiated and differentiated cells (*11*). Moreover, the levels of Fyn expression, as assessed through immunoprecipitation, were roughly the same in the 1C11 clone and its differentiated progenies (Fig. 1B). Therefore, the signaling competence of the 1C11 cell line toward PrP^c activation appeared to depend on the conversion of 1C11 cells into either 1C11*/5-HT or 1C11**/NE cells.

Because Fyn is an intracellular protein but PrP^c is anchored to the outer membrane, the PrP^c-dependent signaling mechanism causing Fyn activation is likely to involve intermediate factor(s). To identify candidate proteins, we performed coimmunoprecipitation experiments with antibodies to PrP using metabolically labeled lysates of 1C11*/5-HT or 1C11**/NE cells. In addition to heterogeneously glycosylated PrP^c molecules, two bands of M_w 21 and 22 kD, respectively, were revealed by SDS–polyacrylamide gel electrophoresis (SDS-PAGE) analysis of the precipitates (Fig. 2A). When the samples receive a pre-treatment of enzymatic deglycosylation with N-glycosydase F (PNGase) , the monoglycosylated PrP^c molecules (migrating to 28 to 30 kD) and the highly glycosylated isoforms (migrating as a band spanning 33 to 40 kD) all resolve into a single species of 25 kD. In contrast, p21 and p22 do not shift in molecular weight after PNGase treatment. Microsequence analysis (Fig. 2B) allowed us to unambiguously identify p21 and p22 as caveolin-1β (cav-1β) and caveolin-1α (cav-1α), respectively. These two isoforms of caveolin-1 differ in their respective initiation sites only (*13*).

In the gel analysis of an immunoprecipitate from 1C11 undifferentiated cells, the bands corresponding to p21 and p22 were barely detectable (Fig. 2A). This observation could not be explained by a defect in caveolin-1 expression in 1C11 precursor cells because all cell types studied here express caveolin. The level of caveolin expression, as measured by Western blot, increased only faintly in differentiated cells compared with 1C11 cells (Fig. 2C). The capacity of PrP^c to interact with caveolin-1 therefore appeared to depend on the differentiation of 1C11 cells toward either a serotonergic or a noradrenergic program.

To assess whether caveolin-1 takes part in the PrP^c-mediated Fyn activation, we introduced antibodies to caveolin-1 to 1C11*/5-HT or 1C11**/NE cells before PrP^c cross-linking with the use of the cell bombardment technique (*14*). Immunosequestration of caveolin-1 in live cells blocked the PrP^c-dependent activation of Fyn (Fig. 2D). Thus, caveolin-1 appears to be one of the protagonists involved in PrP^c coupling to the tyrosine kinase Fyn. Antibodies to clathrin, which were used as a control, were unable to cancel the Fyn response (Fig. 2D), although the amplitude of Fyn activation was somewhat reduced under these conditions. Such a partial reduction

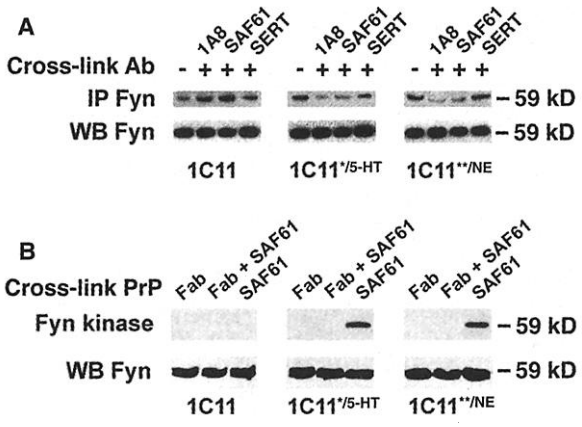

Fig. 1. Immunoprecipitation (IP) and Western blot (WB) of the tyrosine kinase Fyn after antibody-mediated cross-linking in 1C11 precursor, 1C11*/5-HT and 1C11**/NE cells. Cells were incubated overnight at 4°C with 10 μg/ml of antibodies to PrP (1A8 or SAF61, which recognizes the mouse PrP epitope 142-160), Fab fragments of SAF61 antibodies alone or in competition with SAF61 antibodies, or antibodies to the serotonin transporter (SERT), and then were incubated with secondary antibody for 3 hours at 4°C. Cells were activated through incubation at 37°C for 30 min. **(A)** Fyn immunoprecipitation was performed 10 min after cross-linking using FYN-3 antibody (Santa Cruz) as described (*10*). Cells were metabolically labeled with [^{32}P]–γ-ATP (adenosine triphosphate) before lysis to measure the level of Fyn phosphorylation. **(B)** Fyn kinase autophosphorylation assay was performed on immune complexes as in (*16*) before SDS-PAGE analysis. In both panels, Fyn immunoprecipitates were immunoblotted and probed with antibodies to Fyn.

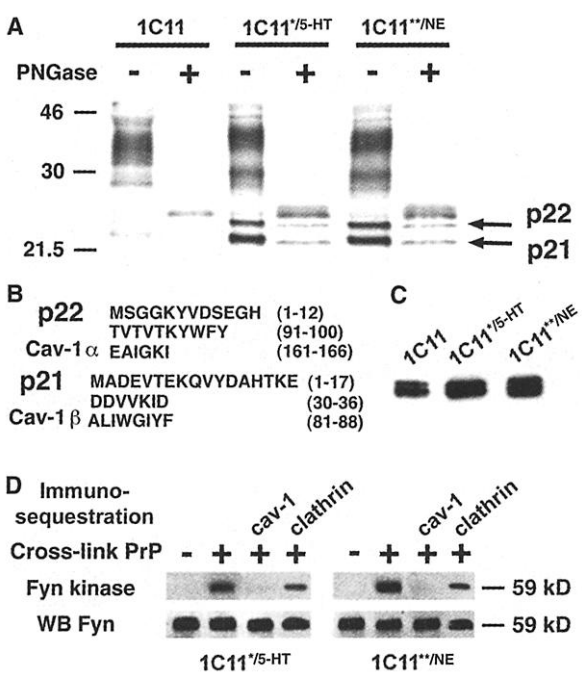

Fig. 2. Functional interaction of PrP^c with caveolin-1. **(A)** Immunoprecipitation and SDS-PAGE analysis of [^{35}S]–metabolically labeled lysates of 1C11 precursor, 1C11*/5-HT, and 1C11**/NE cells with antibodies to PrP was performed as in (*10*). When indicated, samples were treated with PNGaseF to remove Asn-linked oligosaccharides. The experiment was performed at day 4 and day 12 of the serotonergic and noradrenergic programs, respectively. Similar patterns were observed from day 2 of either differentiation. **(B)** For microsequence analysis of p21 and p22, protein from the 1C11*/5-HT immunoprecipitate (about 500 ng) was separated through two-dimensional gel electrophoresis. Excised spots digested with endoproteinase Lys-C were microsequenced using standardized procedures (*17*). **(C)** Immunoblot analysis of caveolin-1 expression in 1C11, 1C11*/5-HT, and 1C11**/NE cells, using C13630 antibodies (Transduction Laboratories, Lexington, Kentucky). **(D)** Cell bombardment with tungsten microprojectiles coated with antibody to caveolin-1 (*14, 18*) abolished the Fyn response to PrP^c activation in 1C11*/5-HT (day 4) and 1C11**/NE (day 12) cells. Immunosequestration of clathrin using excess concentration of antibody to clathrin is also shown as a control experiment.

upon clathrin immunosequestration may reflect indirect interference with the caveolin-dependent signaling pathway through changes in membrane properties. However, it may also indicate a direct involvement of clathrin in the PrP^c-mediated signal.

The difference in signaling competence of 1C11 versus $1C11^{*/5\text{-}HT}$ and $1C11^{**/NE}$ cells prompted us to examine whether the response to PrP^c cross-linking was related to the sequential acquisition of neurotransmitter-associated functions. PrP^c cross-linking was applied at specific time points during each differentiation program. Antibody-mediated ligation of PrP^c failed to induce any activation of the tyrosine kinase Fyn by day 2 of either program (Fig. 3A). Because neurite outgrowth and the onset of neuronal markers are seen as early as 1 day after either induction, simple engagement of 1C11 cells in a neural-like program was not sufficient to confer responsiveness to PrP^c stimulation. Instead, not until day 4 of the serotonergic and day 12 of the noradrenergic differentiation programs were the signaling cascades triggered by PrP^c cross-linking (Fig. 3A). Thus, full differentiation of 1C11 cells and the induction of a functional bioaminergic uptake are a prerequisite for responsiveness to PrP^c activation.

Because the two identified partners of the cascade (Fyn and caveolin) are available in the cells from the beginning of differentiation, several hypotheses can be made. First, PrP^c signaling may involve other yet-to-be-identified cellular partner(s) whose expression is strictly related to the differentiation stage of the cells. Second, the interaction of all cellular partners within a signaling complex may depend on the overall acquisition of neuronal and neurotransmitter-associated functions, specific to the ultimate stage of differentiation. Because caveolin-1 appears to interact with PrP^c from day 2 of either the serotonergic or the noradrenergic program (Fig. 2A), it may be that the recruitment of Fyn to the PrP^c–caveolin-1 complex occurs only at terminal stages of differentiation. Third, the onset of the overall functions of bioaminergic neurons may be a prerequisite to the proper structural organization of the signaling partners within subcellular compartments or microdomains.

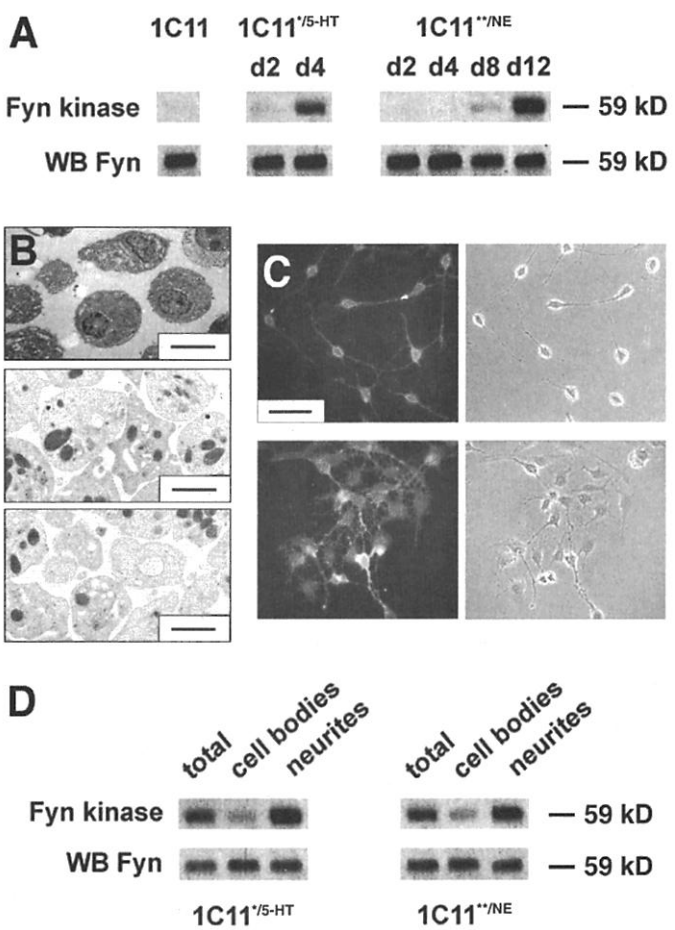

Fig. 3. Relation between the signaling competence of the 1C11 cell line toward PrP^c cross-linking and the onset of neuron- and neurotransmitter-associated functions. In (**A**), Fyn immunoprecipitation was carried out after PrP^c cross-linking, at given times of either differentiation program of 1C11 cells. Immunoprecipitates were subjected to in vitro kinase assay (top) or immunoblotted and probed with antibodies to Fyn (bottom). D2, day 2; d4, day 4; d8, day 8; d12, day 12. (**B**) Cell fractionation and microscopy of fully differentiated $1C11^{*/5\text{-}HT}$ and $1C11^{**/NE}$ cells. Shown are cell bodies of $1C11^{*/5\text{-}HT}$ cells (top panel) and neurite/nerve growth cone fractions of $1C11^{*/5\text{-}HT}$ (middle panel) and $1C11^{**/NE}$ (bottom panel) cells, prepared according to (*19*) before electron microscopy analysis. Bars, 6 μm (top panel) and 1 μm (middle and bottom panels). (**C**) Cell surface immunolabeling of PrP^c in $1C11^{*/5\text{-}HT}$ cells (day 4, top left panel) and of $1C11^{**/NE}$ cells (day 12, bottom left panel) was performed as in (*10*). Phase contrast images are shown in the corresponding right panels. Bar, 70 μm. (**D**) The induction of Fyn catalytic activity after PrP^c cross-linking was measured in cell bodies and neurites separated through cell fractionation in $1C11^{*/5\text{-}HT}$ (day 4) and $1C11^{**/NE}$ (day 12) cells.

Because of the neuronal polarity of $1C11^{*/5\text{-}HT}$ and $1C11^{**/NE}$ cells, we performed cell fractionation to separate neurite extensions from cell bodies (Fig. 3B) and we evaluated the relative contributions of either compartment to PrP^c signaling. In $1C11^{*/5\text{-}HT}$ and $1C11^{**/NE}$ cells, PrP^c was abundant at the surface of cell bodies. Prion proteins were also clustered along the neurites (Fig. 3C). The fraction of PrP^c located at the cell body only weakly contributed to the activation of Fyn upon antibody-mediated ligation (Fig. 3D). In contrast, cross-linking of neuritic PrP^c induced a marked increase in Fyn kinase activity. The amplitude of the response was similar to that observed with total cell lysates (Fig. 3D). In $1C11^{*/5\text{-}HT}$ serotonergic and $1C11^{**/NE}$ noradrenergic cells, the signaling activity of PrP^c may essentially be attributable to those PrP^c molecules located on neurites.

Thus, in the differentiating 1C11 cell system, coupling of PrP^c to the tyrosine kinase Fyn is closely related to the maturation of the cells. Neurotransmitter-associated functions, as well as the structural morphology of the cells, appear to be involved. It is likely that the sequential onset of functional bioaminergic receptors and transporters is accompanied by a spatial organization of membrane components within specialized domains, possibly including cell-surface receptors, membrane adaptators, and signaling molecules. How could this PrP^c-dependent signal functionally interact with other transduction pathways or contribute to cell homeostasis? Brief exposure of fully differentiated $1C11^{*/5\text{-}HT}$ or $1C11^{**/NE}$ cells to antibodies to PrP does not induce any noticeable morphological change. PrP^c is not required for the expression of a critical cell function (*3*). Instead, PrP^c may be involved in the modulation of neuronal functions at the cellular level.

The identification of PrP^c as a signaling molecule opens new directions for unraveling PrP^c function. It also implies the existence of extracellular signal(s) capable of triggering the activation of this protein and provides a foundation for uncovering such signal(s). In the context of prion infection, an important question to resolve is how PrP^{Sc} accumulation may interfere with the signaling activity of PrP^c. The 1C11 cell system, which supports prion replication in vitro (*15*), may help to illuminate this issue.

References and Notes

1. S. B. Prusiner, *Proc. Natl. Acad. Sci. U.S.A.* **95**, 13363 (1998).
2. H. A. Kretzschmar, S. B. Prusiner, L. E. Stowring, S. J. DeArmond, *Am. J. Pathol.* **122**, 1 (1986).
3. A. J. Raeber *et al.*, *Brain Pathol.* **8**, 715 (1998).
4. D. Shmerling *et al.*, *Cell* **93**, 203 (1998).
5. J. P. Brockes, *Curr. Opin. Neurobiol.* **9**, 571 (1999).
6. J. Herms *et al.*, *J. Neurosci.* **19**, 8866 (1999).

7. R. Rieger, F. Edenhofer, C. I. Lasmezas, S. Weiss, *Nature Med.* **3**, 1383 (1997).
8. I. Štefanova, V. Hořejší, I. J. Ansotegui, W. Knapp, H. Stockinger, *Science* **254**, 1016 (1991).
9. S. Mouillet-Richard *et al.*, *J. Biol. Chem.* **275**, 9186 (2000).
10. S. Mouillet-Richard, I. Laurendeau, M. Vidaud, O. Kellermann, J. L. Laplanche, *Microbes Infect.* **1**, 969 (1999).
11. S. Mouillet-Richard, data not shown.
12. S. M. Thomas and J. S. Brugge, *Annu. Rev. Cell Dev. Biol.* **13**, 513 (1997).
13. P. E. Scherer *et al.*, *J. Biol. Chem.* **270**, 16395 (1995).
14. T. M. Klein, E. D. Wolf, R. Wu, J. C. Sanford, *Nature* **327**, 70 (1987).
15. N. Nishida *et al.*, unpublished data.
16. E. M. Kramer, C. Klein, T. Koch, M. Boytinck, J. Trotter, *J. Biol. Chem.* **274**, 29042 (1999).
17. Single-letter abbreviations for the amino acid residues are as follows: A, Ala; C, Cys; D, Asp; E, Glu; F, Phe; G, Gly; H, His; I, Ile; K, Lys; L, Leu; M, Met; N, Asn; P, Pro; Q, Gln; R, Arg; S, Ser; T, Thr; V, Val; W, Trp; and Y, Tyr.
18. A. L. Gainer, G. S. Korbutt, R. V. Rajotte, G. L. Warnock, J. F. Elliott, *Transplantation* **61**, 1567 (1996).
19. K. Sobue and K. Kanda, *Neuron* **3**, 311 (1989).
20. Supported by grants from the Programme de recherche sur les ESST et les prions. We are greatly indebted to Z. Lam, V. Mutel, and J. G. Richards for outstanding experimental support and fruitful discussion. We are grateful to M. Buhler for technical assistance. C. Farquhar kindly provided 1A8 polyclonal antibodies, and SAF61 antibodies were raised at the Service de Pharmacologie et d'Immunologie (CEA, Saclay, France). S.M.R. is a member of the Direction générale de l'alimentation, Ministère de l'Agriculture et de la Pêche.

20 April 2000; accepted 26 July 2000

A Link Between RNA Interference and Nonsense-Mediated Decay in *Caenorhabditis elegans*

Mary Ellen Domeier,[1] Daniel P. Morse,[2] Scott W. Knight,[2] Michael Portereiko,[1] Brenda L. Bass,[2] Susan E. Mango[1]*

Double-stranded RNA (dsRNA) inhibits expression of homologous genes by a process involving messenger RNA degradation. To gain insight into the mechanism of degradation, we examined how RNA interference is affected by mutations in the *smg* genes, which are required for nonsense-mediated decay. For three of six *smg* genes tested, mutations resulted in animals that were initially silenced by dsRNA but then recovered; wild-type animals remained silenced. The levels of target messenger RNAs were restored during recovery, and RNA editing and degradation of the dsRNA were identical to those of the wild type. We suggest that persistence of RNA interference relies on a subset of *smg* genes.

Epigenetic silencing by dsRNA is a widespread phenomenon for regulating gene expression (*1*, *2*). This process, termed RNA interference, or RNAi, is thought to involve targeted degradation of homologous mRNAs (*3*–*7*). In *C. elegans*, seven genes have been shown to be important for RNAi: the *RNA-directed RNA polymerase* homolog *ego-1* (*8*), *mut-7* (*9*, *10*), *rde-2*, *rde-3*, *rde-4*, *mut-2*, and *rde-1*, which encodes a member of the *eIF2c/zwille* family (*10*). At present, it is unclear how the products of these genes function in RNAi, why some of the genes are required for silencing in the germ line but not the soma, or what roles the genes play in other processes such as transposition (*8*–*11*).

Based on the observation that both RNAi and nonsense-mediated decay involve RNA degradation, we examined whether proteins required for nonsense-mediated decay also functioned during RNAi. Seven *smg* genes have been identified, each of which is involved in nonsense-mediated decay (*12*, *13*). Mutations in five of these genes produce identical phenotypes, emphasizing that the SMG proteins act in a common pathway [*smg-1* through *smg-5* (*12*, *14*)].

To compare the effects of RNAi in wild-type (WT) and *smg* animals, we injected dsRNA corresponding to the *unc-54* gene, which encodes myosin heavy chain B and is expressed in body wall muscles (*15*). We chose *unc-54* because it generates a robust RNAi phenotype in which animals are paralyzed (*16*) and also because the severity of paralysis correlates with mRNA levels (*14*, *17*).

We observed that mutant *smg-2* animals recovered rapidly from *unc-54* RNAi-induced paralysis, whereas WT worms did not (Fig. 1A) (*18*). Progeny of injected mothers were examined daily for 4 days after injection. On days 1 and 2, both WT and *smg-2* larvae were severely paralyzed. However, *smg-2* mutants showed increased motility as they aged and moved almost as well as uninjected controls by day 4. We also observed recovery from RNAi in *smg-2* mutants carrying a *sur-5::GFP* transgene (Fig. 1B) (*18*). Thus, recovery was not specific to *unc-54* RNA or to body wall muscles, but occurred in many cell types and for at least two transcripts. GFP expression also rebounded in the neurons of WT worms, indicating that neurons have an intrinsic recovery mechanism that is independent of the *smg* genes.

To rule out the possibility that *smg-2* mutants recovered from RNAi for nonspecific reasons, such as being poor injection hosts, we injected *smg-2*(+/−) heterozygous mothers with *unc-54* dsRNA, scored recovery of individual offspring on day 3, and then determined the genotype of each scored animal. We found that progeny that failed to recover were rarely *smg-2* homozygotes (12% of paralyzed animals, $n = 158$). Conversely, siblings that recovered from RNAi were often *smg-2* homozygotes (55% of moving animals, $n = 131$). If segregation were random, 25% of paralyzed or moving animals would be expected to be *smg-2* homozygotes. These experiments demonstrate that recovery from RNAi depends on *smg-2* activity in the zygote and therefore does not reflect the inability of *smg-2* mutants to function as good injection hosts.

To examine whether *smg-2* mutations affected RNAi-mediated mRNA degradation, we measured endogenous RNA levels using a real-time semiquantitative reverse transcriptase–polymerase chain reaction (RT-PCR) assay (*19*, *20*). Controls with WT and mutant *unc-54* animals demonstrated that our assay accurately reflected transcript levels (*21*). Furthermore, *smg-2* mutations altered *unc-54* RNA levels in ways that paralleled the phenotypic recovery. In WT larvae, *unc-54* RNA levels were reduced about 10-fold compared with uninjected controls and remained low throughout the time course. In *smg-2* animals, *unc-54* levels were reduced 10-fold on day 1, but rebounded rapidly, eventually reaching levels close to those of uninjected controls (Fig. 2). The reduction seen on day 1 was comparable to that seen in WT worms, indicating that the initial response was robust. These data demonstrate that *smg-2* mutants attenuate RNAi-mediated mRNA degradation.

Our data predict that for the effects of the *smg* genes on RNAi to be observed, the targeted mRNA must be transcribed continuously and RNAi must not induce lethality, or the animals will not be able to recover. These requirements explain why recovery in *smg* mutants was not observed previously (*7*). Earlier studies targeted *mex-3*, which is maternally transcribed and essential for embryogenesis (*22*). In addition, these studies assayed *smg-3* mutants, which fail to recover well from RNAi (see below).

[1]Huntsman Cancer Institute Center for Children and Department of Oncological Sciences, University of Utah, Salt Lake City, UT 84112, USA. [2]Department of Biochemistry and Howard Hughes Medical Institute, University of Utah, Salt Lake City, UT 84132, USA.

*To whom correspondence should be addressed. E-mail: susan.mango@hci.utah.edu